5-2020

Discriminating Azo Dyes: Conjugated Polymers, the Inner Filter Effect, and Array Sensors

Erin Crater
University of Southern Mississippi

The University of Southern Mississippi

Discriminating Azo Dyes: Conjugated Polymers, the Inner Filter Effect, and Array Sensors

by

Erin Crater

A Thesis
Submitted to the Honors College of
The University of Southern Mississippi
in Partial Fulfillment
of Honors Requirements

May 2020

Approved by:

_____

Jason Azoulay, Ph.D., Thesis Adviser
Assistant Professor of Polymer Science and Engineering

_____

Derek Patton, Ph.D., Director
School of Polymer Science and Engineering

_____

Ellen Weinauer, Ph.D., Dean
Honors College

Abstract

Azo dyes are abundant pollutants that contaminate water supplies and threaten humans, biota, and ecosystem health. Their detection and discrimination are an incredible challenge due to the structural, chemical, and optical similarities between dyes, the complexity of the wastewater environment in which they are found, and their low environmental concentrations. In this work, the inner filter effect (IFE), combined with conjugated polymer array-based sensing, is utilized for the quantitative profiling of these pollutants. The array was constructed using three fluorescent, anionic conjugated polyelectrolytes whose varying spectroscopic properties led to distinct IFE patterns in the presence of the dyes. The unique fluorescence response patterns were identified and processed using linear discriminant analysis (LDA), enabling the individual identification of 12 closely related azo dyes. To demonstrate its potential in environmental applications, the array was used to differentiate between these dyes at nanomolar concentrations in water.

Keywords: Sensors, polymers, fluorescence spectroscopy, azo compounds, analytical methods

Dedication

To my parents, grandparents, and sister for their continuous support, I would not have made it through the tough weeks without your refreshing and encouraging phone calls. Thank you.

Acknowledgements

I would like to thank Dr. Marco Bonizzoni and his group from the Department of Chemistry and Biochemistry at the University of Alabama for collaboration on this project, and for facilitating the sensor array aspect of this work. I cannot extend enough appreciation to my advisor Dr. Jason Azoulay for the countless opportunities I was given in his research group. The Azoulay Group provided excellent mentors, including my graduate mentor Joshua Tropp. His creativity and passion for science provided the platform for all chemical sensing projects, which gave me the opportunity to complete this thesis work.

I would like to thank the Honors College and Dean Weinauer, whose support from my first semester at USM empowered me to dream big. Additionally, I pay special thanks to the professors that made the classroom my favorite place to be (Dr. Storey, Dr. Pigza, Dr. Schroeder, and countless others), thank you for serving as my role models. I left your classes wishing I could learn more, so my decision to pursue a Ph.D. can be largely attributed to you. To Dr. Joseph Lott, thank you for giving me the opportunity to complete research in your group as a freshman and for encouraging me through the learning curve of working in a laboratory. I owe a special thank you to Dr. Heather Broadhead for working tirelessly for us undergraduates, and for making my double major possible.

Table of Contents

List of Tables .....**Error! Bookmark not defined.**

List of Figures .....**Error! Bookmark not defined.**x

List of Abbreviations .....**Error! Bookmark not defined.**

Chapter 1: Introduction .....**Error! Bookmark not defined.**

Chapter 2: Literature Review 3

Wastewater effluent and azo dyes 3

Conjugated polymers and the inner filter effect 4

Sensor arrays 6

Chapter 3: Methods 8

Synthetic methods 8

Optical experiments 9

Chapter 4: Results and Discussion .....**Error! Bookmark not defined.**

Physical characterization and optical properties of polymers**Error! Bookmark not defined.**

Inner filter effects .....**Error! Bookmark not defined.**

Sensor array .....**Error! Bookmark not defined.**

Mechanism of quenching .....**Error! Bookmark not defined.**

Chapter 5: Conclusion 22

References 23

List of Tables

Table 1. Molecular weight and dispersity characterization of **P1**-**P3**..... 12

Table 2. Fluorescence lifetime decay of each component for **P1**-**P3** and CR. 20

List of Figures

Figure 1. Diagram of the inner filter effect.....**Error! Bookmark not defined.**

Figure 2. Synthetic scheme of **P1**-**P3**.....**Error! Bookmark not defined.**

Figure 3. Absorption spectra and structures of azo dyes and fluorescence of **P1**-**P3**..... 13

Figure 4. Optical overlap of **P2** and CR and titration of **P2** with CR..... 14

Figure 5. Limits of detection of **P1**-**P3** upon titration of CR..... 16

Figure 6. Scores and loadings plots of processed assays with and without **P1**-**P3**..... 18

Figure 7. Additive lifetime and absorption plots and LOD curves..... 21

List of Abbreviations

AO	Acid Orange
AR	Acid Red
CP	Conjugated Polymer
CPE	Conjugated Polyelectrolyte
CR	Congo Red
DI	Deionized
DMF	*N,N*-dimethylformamide
FRET	Förster Resonance Energy Transfer
GC-MS	Gas Chromatography – Mass Spectrometry
GPC	Gel Permeation Chromatography
HPLC	High-Performance Liquid Chromatography
IFE	Inner Filter Effect
LDA	Linear Discriminant Analysis
LOD	Limit of Detection
LOQ	Limit of Quantification
MALLS	Multi-angle Laser Light Scattering
M_n	Number Average Molecular Weight
PAH	Polycyclic Aromatic Hydrocarbon
PCA	Principal Component Analysis
$Pd(PPh_3)_4$	Tetrakis(triphenylphosphine)palladium(0)
pIFE	Primary Inner Filter Effect
sIFE	Secondary Inner Filter Effect
SYFCF	Sunset Yellow SCF
TCSPC	Time-correlated Single-photon Counting
THF	Tetrahydrofuran
USM	University of Southern Mississippi
UV	Ultraviolet
UV-Vis	Ultraviolet-Visible
Vis	Visible
ε	Molar Extinction Coefficient
$Đ$	Dispersity

Chapter 1: Introduction

The world population nearly tripled from 1.65 billion to 6 billion people during the 20th century, and is now approaching 8 billion people. With this dramatic increase, as well as a global rise in standard of living, crises revolving around sustainability have developed as important concerns. The interconnected nature of human health, environmental pollution, climate change, and water demand require a more conscious stewardship of our resources, and a more complete understanding of their life cycle, circulation, and long-term effects. The limited information available regarding the quality of our water sources remains a key challenge to these efforts as the identity, toxicology, and circulation of contaminants in rivers, lakes, oceans, etc. act as knowledge gaps, providing an inadequate description of our environment.

The activities and assessments required to characterize the quality of the environment are referred to as environmental monitoring. These efforts allow for an empirical assessment of the impact of human activity, providing statistical analysis, publication through peer review, and a historical record to enable small and large scale modeling.[1] Most tasks related to environmental monitoring involve tracking chemical substances that have a harmful effect on the environment and various organisms. Valuable information about air, soil, and water quality can be extracted from information regarding the concentration and circulation of these pollutants.[2]

Broadly defined, water quality is the chemical and biological characteristics of water.[3] Federal agencies are guided by quantitative standards determined by researchers for the assessment of water quality. Sampling can be achieved through various techniques including grab sampling manually with a clean bottle or mechanically with a rosette

sampler, automated sampling stations, passive sampling, and remotely using aerial platforms.[4,5] Analytical techniques such as spectrophotometry, chromatography, spectrometry, and electrochemistry provide reliable information for a wide range of pollutants. However, such techniques lack portability and require time consuming sample preparation procedures, which limit most water quality monitoring technologies to detecting pH, dissolved oxygen, conductivity, temperature, and color.[6,7] Technologies for the on-site detection of other important pollutants are not widely available. The work described in this thesis aims to contribute to the field of chemical sensing by developing methods to detect and discriminate between 12 hazardous and closely related azo dyes, which are toxic organic compounds that are indiscriminately disposed into wastewater.[8]

Chapter 2: Literature Review

Wastewater effluent and azo dyes

Azo dyes are an abundant class of synthetic small molecules accounting for more than half of dyes produced worldwide. These dyes are primarily used as colorants of textiles and as plastic additives.[8] Because the dyes do not completely bind to the fibers, the free dyes have the potential to be released into the environment. It is estimated that 10% of dyes produced are released as effluents, classifying wastewater from textile plants as the most polluting of all industries.[8] Additionally, the stability of these compounds prevents them from being easily removed during common wastewater treatment methods. Azo dyes are characterized by the diazo group (C-N=N-C), often linked to phenyl or napthyl groups and substituted with various functional groups such as sulfate or hydroxyl chemistries. The diazo group within these dyes readily reduces to hydrazine and aromatic amine containing compounds, which are extremely hazardous to human health.[9] Many azo dyes have been found to pose carcinogenicity, genotoxicity, and mutagenicity, making the disposal of these dyes a major threat to animals, the environment, and the world at large.[9] For example, Congo Red (CR) a benzidine based dye, has been banned in many countries due to its carcinogenicity.[9] Efforts to study the transport and toxicity of these compounds are rapidly growing; however, this continues to be a major technological hurdle due to the large number of possible dyes, the combined use of several dyes in industrial applications, and low active concentrations in the environment. Common analytical techniques to detect these compounds include chromatographic methods such as gas chromatography coupled to mass spectrometry (GC-MS), high-performance liquid chromatography (HPLC), and liquid chromatography coupled to mass

spectrometry (LC-MS). While highly sensitive, these methods generally focus on the dye metabolites rather than the azo dye pollutants, making their source difficult to trace.[10-12]

Conjugated polymers and the inner filter effect

Fluorescence remains a leading signal transduction method for chemical sensors due to high sensitivity, ease of operation, and broad applicability. Optical sensors are promising for on-site measurements where a handheld spectrophotometer can easily be transported and extensive training for operation is not required. Fluorescent sensors based on conjugated polymers (CPs) are advantageous over small molecule fluorophores as their delocalized electronic structure leads to large molar extinction coefficients, strong fluorescence, and signal amplification through the "molecular wire effect."[13] This effect often relies upon receptor chemistries which are tethered to the polymer to bind a particular analyte. The local interactions between the receptor unit and the analyte are relayed through the "molecular wire" of the conjugated backbone, amplifying the signal by orders of magnitude compared to analogous small molecule sensors.

Although the diverse methods for signal transduction in fluorescent CP-based sensors have enabled the sensitive and selective detection of many analytes, there are several limitations in currently utilized mechanisms when considering a sensing technology that can be used in environmental conditions. Most methods rely on supramolecular host/guest chemistries and their associated noncovalent interactions. However, supramolecular chemistries are commonly designed to operate in nonpolar media and attempts to transfer rules for molecular recognition into water have proven to be not trivial.[14] The main challenge is related to the highly competitive solvation of environmental pollutants in water, as many of the pollutants are ionic. As such,

recognition of these contaminants generally requires strong Coulomb or coordinative interactions rather than hydrogen bonding.[15] Other challenges include the lack of available recognition elements for particular analytes of interest, or the complexity of coupling the receptor to an analyte-driven response. Once a host/guest chemistry is coupled to the CP, similar analytes may also trigger the fluorescence response, limiting the selectivity of the optical sensor. For these reasons, most published CP-based sensors operate in nonpolar media, detect a single analyte, and only slightly deviate from previous literature examples.

The inner filter effect (IFE) is an optical phenomenon that circumvents the need for tailored host-guest interactions by taking advantage of the intrinsic optical properties of a fluorescer and absorber.[16] The process involves an absorbing species that competes with another fluorescent species for light, resulting in a decrease of the fluorescence intensity of the fluorescer, also known as apparent quenching. When overlap of the

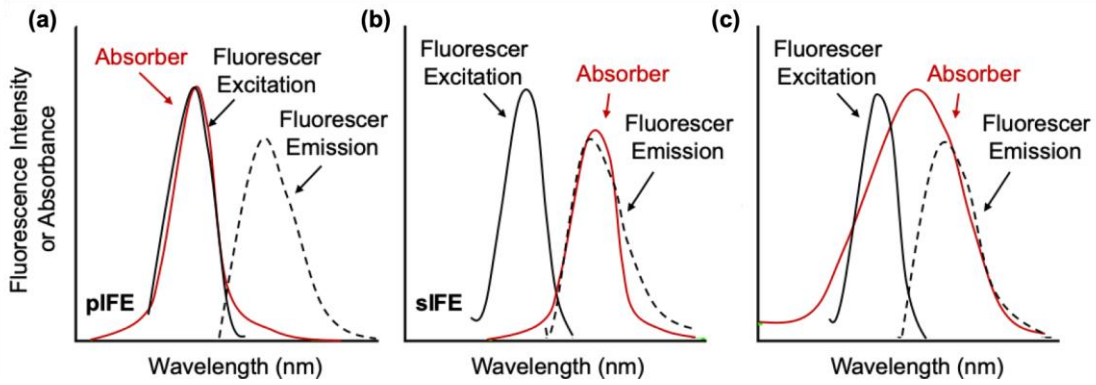

Figure 1. The inner filter effect where the absorption spectrum of absorber overlaps with (a) the excitation spectrum of the fluorescer, (b) the emission spectrum of the fluorescer, or (c) both. (Adapted from Ref. 16, abstract)

absorption of the absorber and fluorescer is high, the IFE will take place (Figure 1). Overlap of the absorber with the absorbance of the fluorescer is known as the primary IFE (pIFE, Figure 1a), whereas overlap of the absorber with the emission of the

fluorescer is known as the secondary IFE (sIFE, Figure 1b). The IFE can be applied to sense analytes that do not possess molecular handles for available receptor chemistries. Recently, a conjugated polymer based on fluorene has been demonstrated as a sensor through the IFE for picric acid, a nitroexplosive compound.[17] Titration of the polymer (fluorescer) with picric acid (absorber) resulted in apparent quenching of the polymer's fluorescence, leading to a limit of detection in the low micromolar range. More recently, the IFE was used to detect Sudan dyes, a class of highly carcinogenic azo compounds.[18] The authors formed fibrous membranes and films from poly(vinyl alcohol), and tethered fluorophores that possessed spectral overlap with the Sudan dyes. Though they were able to detect the dye at relatively low concentrations, the method still suffered from poor discrimination as through the inner filter alone, similar analytes demonstrated false-positive results.

Sensor arrays

Recently, array-based sensing has been demonstrated as a technique to sense structurally and chemically similar analytes through multivariate pattern recognition.[19] Principal component analysis (PCA) and linear discriminant analysis (LDA) are statistical methods that use a linear combination of variables to best represent data. These pattern recognition algorithms can distinguish features in large data sets and for this reason, are commonly used in the classification of data. One feature that could be classified through these methods is fluorescence quenching. For example, fluorescent polymers that possess varying degrees of optical overlap with analytes are quenched differentially; *the greater the spectral overlap, the greater the quenching.* When applied to chemical sensing, the small differences in fluorescence quenching can be processed

using statistical analyses such as LDA.[19] In our group, this method has been used to discriminate between sixteen polycyclic aromatic hydrocarbons (PAHs) using the IFE as the signal transduction pathway.[20] Designing polymers that interfered with the absorption and fluorescence of the PAHs yielded differential quenching that, when processed using LDA and PCA, led to the qualitative discrimination of the PAHs.[20] Scores and loadings plots are obtained from LDA analysis which are used to visualize discrimination. Tight intra-cluster spacing indicates reproducibility and large inter-cluster spacing is representative of discrimination.[20] In the article, the results from the LDA loadings plot showed that the absorbance of the PAHs only slightly contributed to the discrimination, whereas variables such as the fluorescence of the polymers were the most important contributors to the discrimination. Increased reliance on fluorescence signals was desirable as it was hypothesized that the high photoluminescence quantum efficiencies of fluorene-based copolymers would offer considerably lower limits of differentiation for PAHs compared to an array relying primarily on the absorption properties of PAHs. In other words, although the intrinsic absorbance of the PAHs offered some discrimination, complete discrimination of the PAHs was not possible without the polymers.[20] In this body of work, it was hypothesized that designing polymers that interfered with the absorption of 12 azo dyes would induce an IFE that could be leveraged to discriminate between very similar dyes.

Chapter 3: Methods

Synthetic methods

Our studies began by synthesizing a series of anionic conjugated polyelectrolytes (CPEs) based on fluorene copolymer structures with varied conjugated comonomers as shown in Figure 2. Conjugated polymers are typically synthesized through metal-mediated step growth polymerizations, and in this study, the Stille cross-coupling was used as dibromofluorene and the stannane-functionalized monomers were readily available. Anionic butanesulfonate groups were attached as side chains to promote water solubility and to reduce aggregation. Additionally, the multiple negative charges from the sulfonate groups were chosen to minimize direct interactions with negatively charged azo dyes, thus restricting other quenching mechanisms such as Förster resonance energy transfer (FRET*)*, while amplifying effects associated with the IFE.

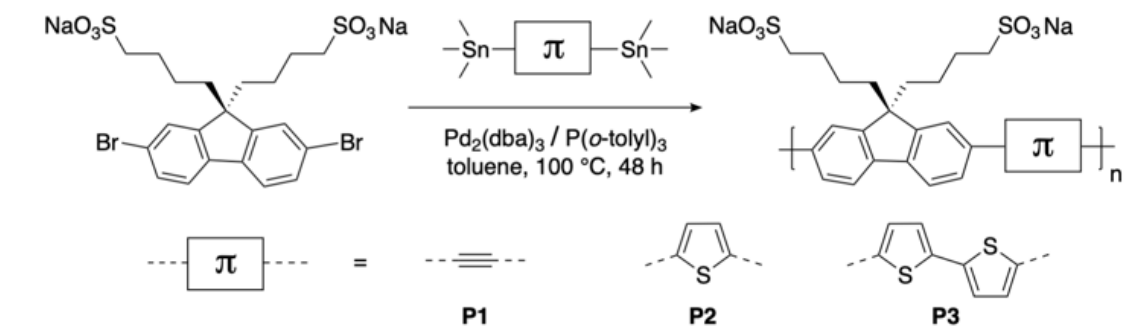

Figure 2. Synthesis of **P1**-**P3**: $Pd_2(dba)_3$ (5.0 mol %), P(o-tolyl)$_3$ (20 mol %), toluene, 100 °C, 48 h.

Reagents were purchased from Sigma-Aldrich and used without further purification. Toluene was degassed and dried over 4 Å molecular sieves. Tris(dibenzylideneacetone)dipalladium(0) ($Pd_2(dba)_3$) was purchased from Strem Chemicals and used without further purification. 2,7-Dibromo-9,9-bis(4-

sulfonatobutyl)fluorene disodium was prepared according to literature procedures.[21] Poly[9,9-bis(4'-sulfonatobutyl)fluorene-*alt*-*co*-ethynyl] (**P1**), poly[9,9-bis(4'-sulfonatobutyl)fluorene-*alt*-*co*-thiophene] (**P2**), and poly[9,9-bis(4'-sulfonatobutyl)fluorene-*alt*-*co*-2,2' bithiophene] (**P3**) were synthesized using a Stille cross-coupling copolymerization between 2,7-dibromo-9,9-bis(4'-sulfonatobutyl)fluorene disodium and bis(stannyl) monomers using a $Pd_2(dba)_3$/P(*o*-tolyl)$_3$ catalyst system in toluene according to previously reported procedures (Figure 2).[22, 23] **P1**-**P3** were purified as previously reported using dialysis in deionized (DI) H_2O to remove low molecular weight starting materials and product. This was followed by lyophilization to dry the samples, which powderized the polymers for simplified manipulation during analytical experiments. The number average molecular weight (M_n) and dispersity ($Đ$) were measured on a Waters Alliance 2695 separations module, an online multiangle laser light scattering (MALLS) detector fitted with a gallium arsenide laser (20 mW) at 658 nm (miniDAWN TREOS, Wyatt Technology Inc.), an interferometric refractometer (Optilab rEX, Wyatt Techhnology Inc) operating at 65 °C, and 685 nm with two PL-Gel Mixed-C columns (Agilent) in series (pore size 50-10^3 Å, 5 μm bead size). The mobile phase corresponded with DMF (1.0% LiBr) delivered at a flow rate of 0.5 mL/min. LiBr was added to the DMF eluent to help dissolve the polymers by taking the place of hydrogen bonds, preventing them from aggregating.

Optical experiments

All optical experiments were performed in DI H_2O. UV-Vis absorption spectra were recorded using an Agilent Technologies Cary 5000 UV-Vis-NIR spectrophotometer in matched 1-cm quartz cells. The molar extinction coefficients of the dyes were

determined through standard Beer's Law titrations. Fluorescence decay profiles were measured using a Horiba PPD850 time-correlated single-photon counting (TCSPC) detector with a Fianium WhiteLase SC-400 laser excitation source at maximum power and a repetition rate of 2 MHz. Lifetime decay measurements of **P1**-**P3** (10 μM) in the absence and presence of CR (15 μM) were performed via pulse excitation at the wavelength of maximum absorption of each polymer and collected at the wavelength of maximum emission.

Steady-state photoluminescence measurements were recorded using a PTI-Horiba QuantaMaster 400 spectrofluorometer equipped with a 75 W Xe arc lamp. All fluorescence spectroscopy experiments were performed in DI H_2O unless otherwise stated. Polymer and dye stock solutions were prepared separately, then 3 mL of the polymer solutions were inserted into a quartz cuvette, and fluorescence spectra were collected for **P1**-**P3**. Fluorescence emission spectra were collected by exciting the polymer at their most red-shifted spectral maximum. Titration experiments were performed by adding aliquots of dye solution to the polymers in 10 μL increments.

Multivariate data was acquired on a BioTek *Synergy II* multimode microwell plate reader, capable of measuring absorption spectra through a monochromator and steady-state fluorescence intensity measurements through a set of bandpass filters. Fluorescence measurements were collected using 26 filter combinations ($\lambda_{exc}/\lambda_{em}$): 330/450 nm, 330/460 nm, 330/485 nm, 330/516 nm, 330/528 nm, 330/560 nm, 330/580 nm, 330/645 nm, 380/450 nm, 380/460 nm, 380/485 nm, 380/516 nm, 380/528 nm, 380/560 nm, 380/580 nm, 380/645 nm, 450/516 nm, 450/528 nm, 450/560 nm, 450/580 nm, 450/645 nm, 460/516 nm, 460/528 nm, 460/560 nm, 460/580 nm, and 460/645 nm.

Absorbance measurements were collected from 300 to 560 nm at 20 nm increments. The sample compartment was temperature controlled at 25 °C. Experiments were manually organized using Eppendorf Research multichannel pipettors and disposable plastic tips into black Greiner BioOne non-treated (medium binding) polystyrene microwell plates with a clear flat bottom for UV absorption and fluorescence spectroscopy in a 384-well configuration. Each well was filled with 100 μL of solution. Plates were read on a multimode plate reader immediately after preparation.

Chapter 4. Results and Discussion

Physical characterization and optical properties of polymers

Polymers **P1**-**P3** were characterized with size exclusion chromatography, providing molecular weight and distribution data shown in Table 1. The dispersity of the polymers is lower than that of typical step growth polymers, which can be attributed to the dialysis step of the polymer workup which removed residual monomer and low molecular weight oligomers.

Table 1. Molecular weight and dispersity characterization of **P1**-**P3**.

	P1	**P2**	**P3**
M_n (kg/mol)	9.3	8.4	10.2
$Đ$	1.8	1.6	1.9

Incorporating the ethynyl (**P1**), thiophene (**P2**), and 2,2'-bithiophene (**P3**) structural units within the copolymer backbone systematically red-shifted the absorption profile of the polymers, giving absorption maxima (λ_{max}) at 365, 413, and 454 nm, respectively (Figure 3a). The emission profiles of the copolymers were also red-shifted with emission maxima (λ_{em}) at 405, 464, and 546 nm, respectively (Figure 3b). These copolymers yielded a series of fluorophores that overlapped with the absorption profiles of the azo dyes differentially (Figure 3d-f).

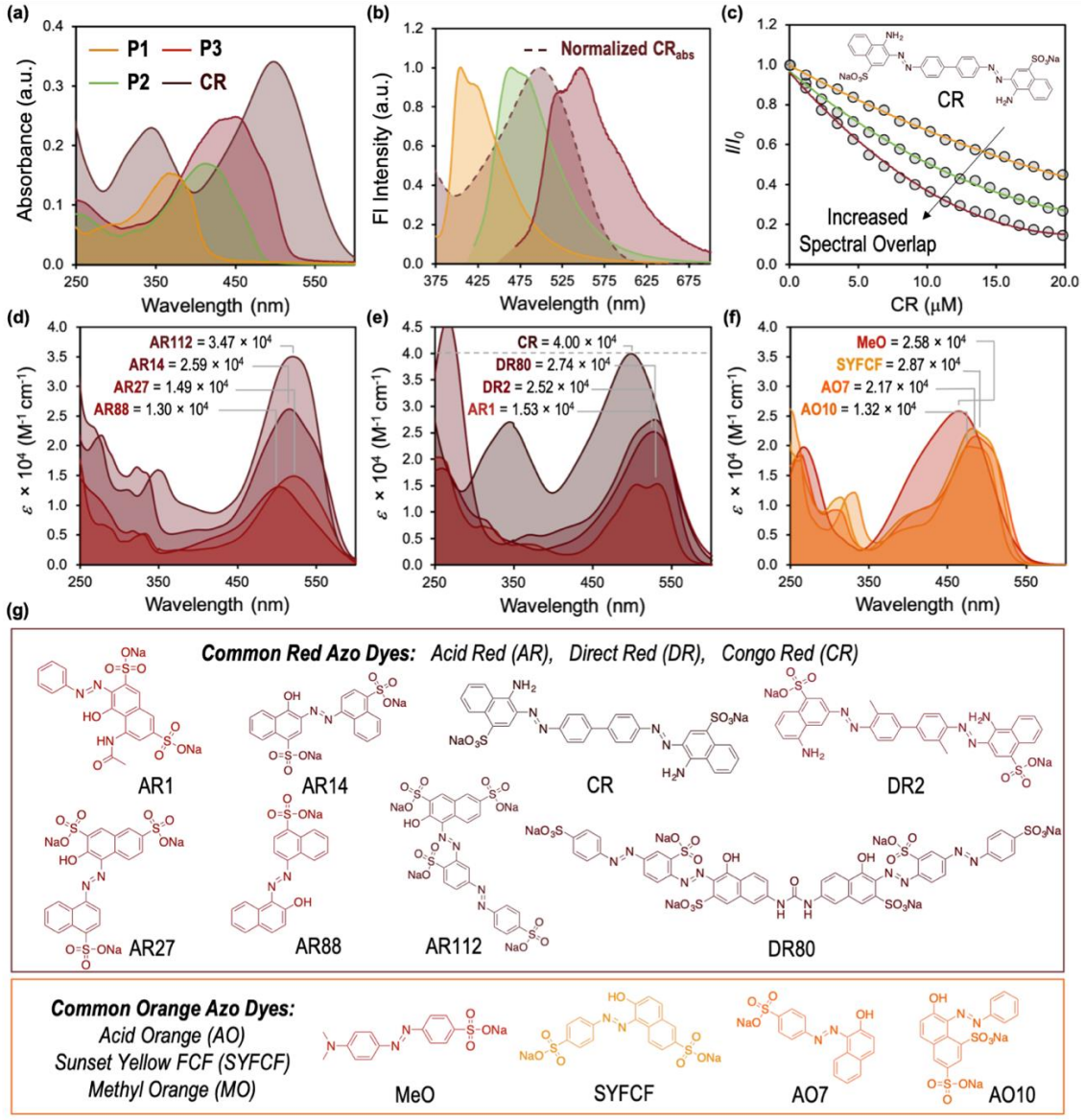

Figure 3. (a) Absorbance spectra of **P1**-**P3** (10 μM) and CR (10 μM). (b) Normalized fluorescence spectra of **P1**-**P3** (10 μM) and the normalized absorption of CR. (c) Maximum fluorescence intensity of **P1**-**P3** upon titration with aliquots of CR. (d-f) Molar absorptivity of the azo dyes in DI H_2O, with extinction coefficients at λ_{max} for each dye. (g) Structures of the azo dyes used in this study.

Inner filter effects

For this study, 12 azo dyes within the same color class (orange – red) were selected for their similar optical properties, and because several of the dyes and/or their byproducts are carcinogenic, genotoxic, and mutagenic (Figure 4g).[24, 25] In Figure 3, the

similarities between the dyes are shown, with the only discernible differences being minor variations in the molar absorptivity (ε) in similar spectral regions. The colors of each dye and associated spectra are matched with the color of the compound in the solution state. The absorbance and emission of **P1**-**P3** falls within the region of dye absorption, offering the opportunity for the pIFE and sIFE to provide differential quenching of these polymers. Quenching of the emission intensity of **P1-P3** was observed through the IFE given by a plot of I/I_o against Congo Red (CR) concentration, where I and I_o are the fluorescence intensities of **P1**-**P3** in the presence and absence of CR, respectively (Figure 3c).

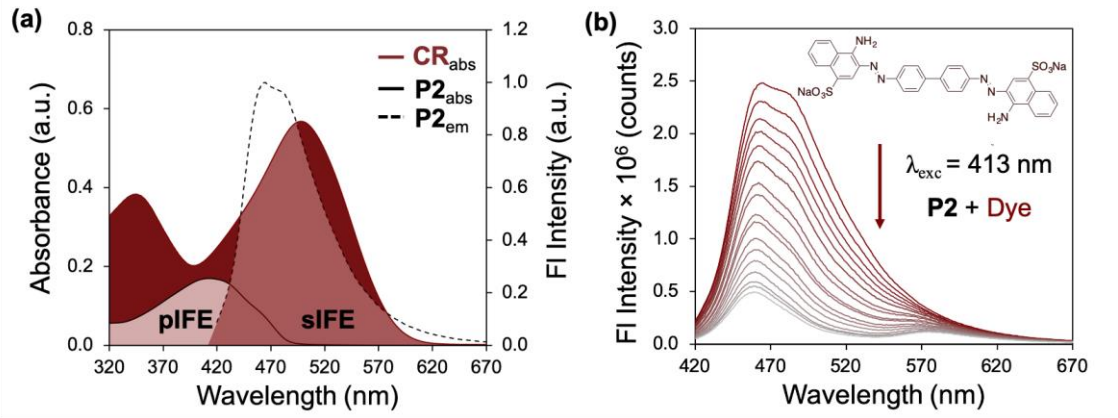

Figure 4. (a) Normalized absorption and emission of **P2** (10 μM) overlaid with CR absorption (15 μM) (b) Fluorescence spectra of **P2** (10 μM) upon titration with CR (0 – 21.9 μM), λ_{exc} = 413 nm.

As an example, the absorption of CR, a carcinogenic azo dye,[26] overlaps with the absorption and emission of **P2**. Titration of the polymer with CR resulted in apparent quenching of the fluorescence of **P2** through the IFE, with CR acting as an effective "filter" of the polymer's fluorescence (Figure 4b). The differential responses arise from the different dependence of the absorption strength (molar extinction coefficient) and fluorescence emission of each polymer and of CR on the wavelength (Figure 3a-b).

Excitation of **P1** at λ_{exc} = 365 nm demonstrated the least efficient quenching (λ_{em} = 405 nm) as a result of the weakest absorbance overlap (pIFE) and emission overlap (sIFE) with CR. **P2** demonstrated the best sIFE with CR, with very good overlap between CR absorbance and **P2** emission signals. However, there was only minor involvement of the pIFE, as the absorbance signals of the CR dye and **P2** did not overlap well. **P3** showed the greatest contributions from both the pIFE and sIFE (λ_{em} = 546 nm), since the absorbance of CR overlapped most significantly with both the absorbance and emission signals of the polymer. Moreover, the optical signals from **P3** overlapped with the most intense region of the CR dye's absorbance (450 – 600 nm). Within this region, **P3** displayed a λ_{max} of 454 nm with $\varepsilon = 2.41 \times 10^4\ M^{-1}cm^{-1}$, greater than the other two polymers. Therefore, **P3** demonstrated the most efficient quenching through the IFE. As a representative example, the limits of detection (LOD) for CR using **P1**-**P3** as sensors were found to be between 0.13 – 1.76 μM (Figure 5). The LOD was calculated as LOD = $3\sigma/k$, where σ was the standard deviation of the y-intercept of the calibration curves and k was the average slope of the calibration curves. **P1** demonstrated the lowest LOD as it had the highest fluorescence intensity, while **P3** demonstrated the highest LOD as it had the lowest fluorescence intensity. The observed low LOD values correspond to low parts-per-million and high parts-per-billion sensitivity, corresponding to an analytically useful range for typical dye concentrations in environmental samples.[25,34-35]

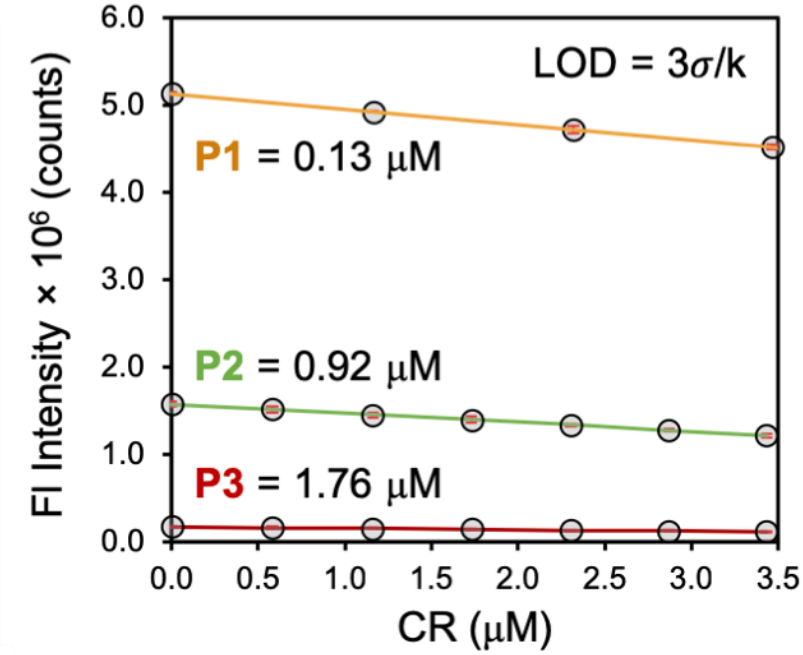

Figure 5. Maximum fluorescence intensity of **P1**-**P3** (10 μM) upon titration with CR in DI H_2O and limits of detection (LOD) labelled. Red error bars represent the standard deviation of three experiments at each concentration.

Sensor arrays

The slight differences in apparent quenching efficiencies of each of the dyes to each polymer provided a discriminatory handle for statistical analysis. The array was formed by organizing 10 μM solutions of **P1**-**P3** on a 384-well microplate and adding aliquots of the 12 dye solutions, bringing the concentration of the dyes to 15 μM in each well. Each dye-polymer combination was prepared in replicates of 14, and a microwell plate reader was used to collect multiple absorbance and fluorescence measurements using the optical filters listed in the *Optical experiments* section. The raw data was processed using LDA in *Mathematica*, where the LDA algorithm transforms the optical dataset (fluorescence and absorption measurements from each well) to generate a new set with descriptor variables (known as factors) that are linear combinations of the original instrumental variables.[27-29] The obtained factors are reported in decreasing order of the

amount of information from the original dataset they contain. This allows for straightforward simplification of the dataset by retaining only the first two factors with minimal loss of information, as most of the original data can be represented by just these two factors. Figure 6a displays the two-dimensional LDA scores plot for the array at a dye concentration of 15 μM. Each dye cluster was well-separated from one another, with tight intra-cluster distances (spacing between similar dyes on the scores plot) indicating excellent reproducibility, and large inter-cluster distances (spacing between dissimilar dyes on the scores plot) indicating good discriminatory power. Of the information present in the original dataset, 83.0% was retained in the first two factors. The factor loadings from the LDA analysis, i.e. the contributions of the original instrumental measurements to the first two factors, indicated that fluorescence measurements from **P2** acted as the most important contributor to the discrimination. In fact, at the excitation/emission wavelengths measured, **P2** displayed the greatest differences in spectral overlap with the absorbance of each dye, compared to that of the other polymers.

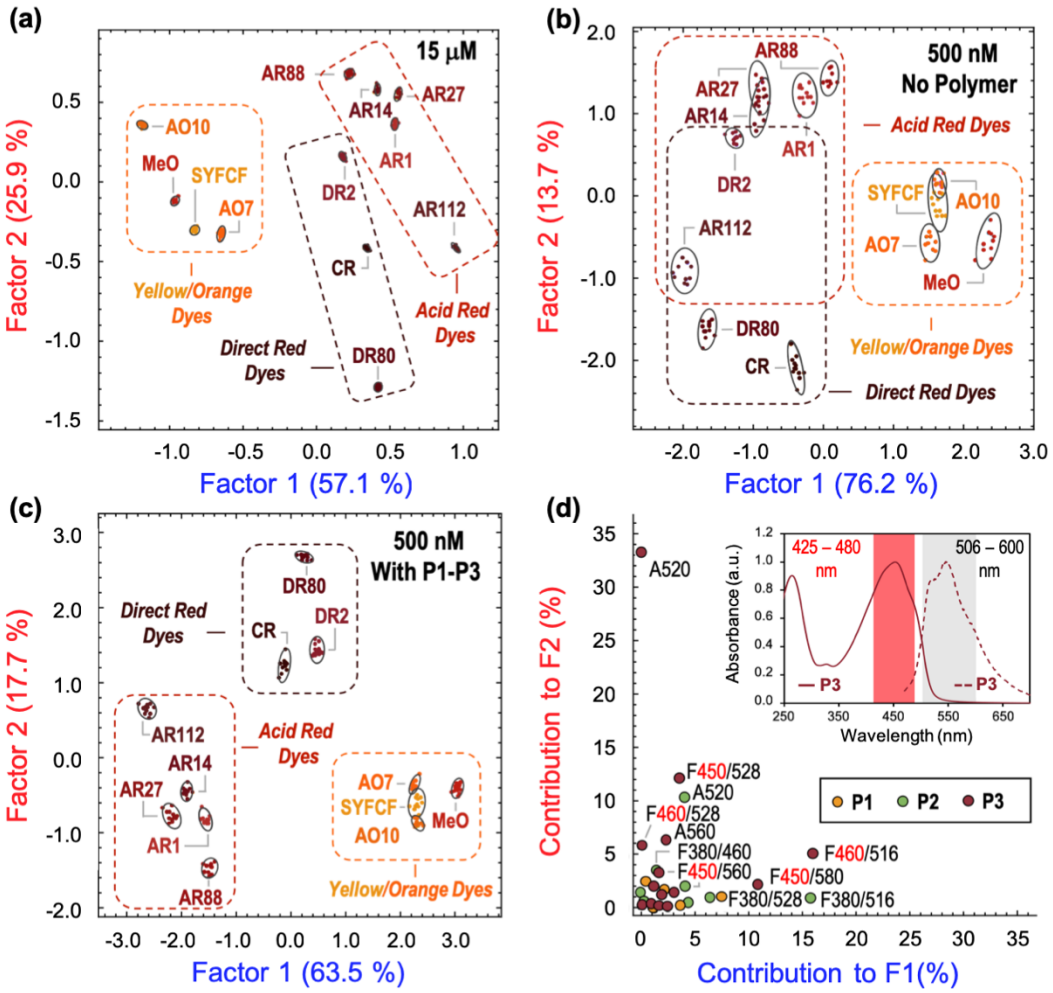

Figure 6. (a) 2D LDA scores plot for the differentiation of 12 azo dyes (15 µM) with **P1**-**P3** (10 µM). (b) 2-D plot of the LDA scores for 12 azo dyes without **P1**-**P3** at 500 nM. (c) 2-D plot of the LDA scores for the differentiation of 12 azo dyes (500 nM) with **P1**-**P3**. (d) LDA loadings plot illustrating the relative contributions of each instrumental variable to the first two LDA factors. Inset: UV-Vis absorption and fluorescence spectra of **P3**, with wavelengths of maximum contribution highlighted.

At much lower dye concentrations commonly encountered in environmental samples such as rivers and wastewater (500 nM),[9] the absorbance signals of the target dyes were no longer detectable. This precluded differentiation based on absorption alone (Figure 6b), which is supported by grouping within their color index. For example, at 500 nM, the closely related red dyes (AR14 and AR27) and yellow/orange dyes (AO10 and SYFCF) cluster together in the LDA scores plot, preventing their individual

identification. However, when incorporating fluorescence measurements from **P1**-**P3**, complete differentiation of all 12 dyes was recovered. Figure 6c displays the corresponding LDA scores plot at 500 nM, where replicates of the same dye sample were found to cluster tightly, and clusters from different samples were clearly separated, indicating excellent reproducibility and strong discriminatory power of the polymer-based array, even at nanomolar dye concentrations. Fluorescence characteristics were the most important contributors to the discrimination (Figure 6d), indicating the prominent role of **P1**-**P3** in the differentiation, since azo dyes are not fluorescent.[30] Fluorescence characteristics from **P3** in particular were the most important to the discrimination at 500 nM, because at such low concentrations any significant absorption from the dyes would occur between 450 and 600 nm, a range which overlaps significantly with the absorption and emission of **P3** (Figure 6d, inset).

Mechanism of quenching

To understand the fluorescence quenching mechanism, steady-state absorption and time-resolved fluorescence measurements were performed. Generally, the mode of quenching relates to the interactions between the absorber and the fluorescer, whereas in the IFE, no direct physical interactions are detected.[31] In an effort to operate solely through the IFE, the interactions were minimized through the intstallment of the anionic sulfonate groups, which would repel the anionic azo dyes. Overlap between the dye absorption spectrum ranging from 200 to 600 nm with the absorption and emission spectra of **P1**-**P3** gives the possibility of Förster resonance energy transfer (FRET),[31] which can occur when two species possess optical overlap, similar to the IFE. The fluorescence lifetime of the polymers was measured in the absence and presence of the

representative dye, CR. Fluorescence lifetime decays of each component are tabulated in Table 2.

Table 2. Fluorescence lifetime decay of each component for **P1**-**P3** and CR.

τ_1 (ns)	**P1**	**P2**	**P3**
Polymer	0.841	0.893	0.525
Polymer + CR	0.788	0.893	0.578

It is evident from Figure 7 that the difference between the emission decay of **P2** in the presence and absence of CR was minimal, which ruled out a dynamic quenching mechanism such as FRET.[17,32,33] The fluorescence lifetimes for **P1** and **P3**, given in Table 2, demonstrated the same behavior. Additionally, the absorption spectrum of a mixture of the polymer and dye was completely additive, which ruled out static quenching from aggregation and formation of a ground-state complex (Figure 7, inset). When these results were considered, the IFE was the most probable mechanism for quenching of the polymer's emission.

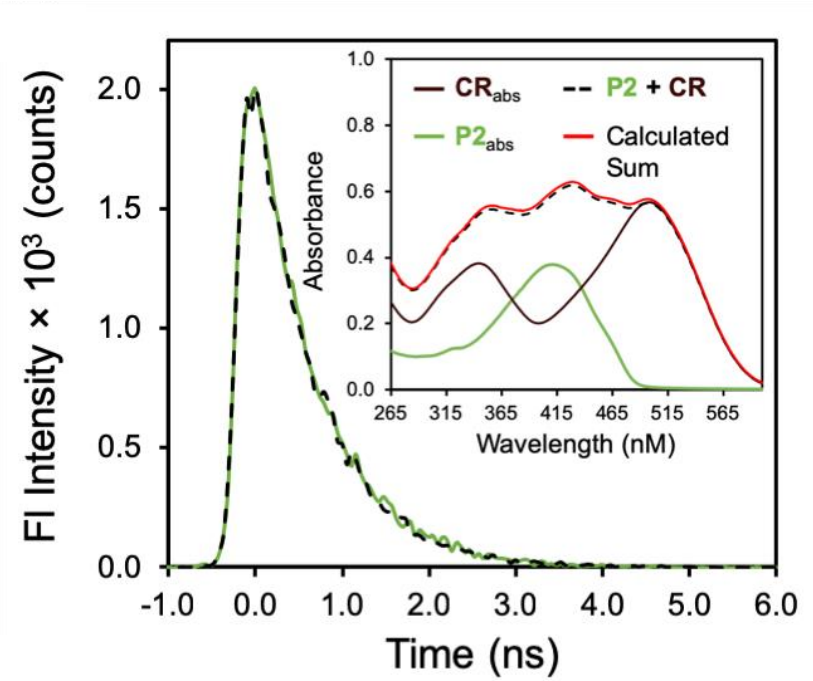

Figure 7. Emission decay of **P2** (10 μM) in the presence and absence of CR (15 μM). Inset: UV-Vis absorption spectra of **P2** (20 μM), CR (15 μM), and of a mixture of **P2** and CR, compared to a simulated spectrum calculated from the sum of the individual experimental spectra.

Chapter 5: Conclusion

In summary, we demonstrated the detection and discrimination of 12 structurally and optically similar azo dyes at parts-per-billion concentrations in an aqueous solution. Three highly fluorescent, water soluble CPEs were prepared with varying spectroscopic overlap with target dyes, providing distinct apparent quenching behavior through the IFE. The differential responses were collected using a microwell plate reader operating under standard spectroscopic techniques, and multivariate pattern recognition strategies were used to interpret the data and to produce two-dimensional score plots which operated as effective calibration plots for the differentiation of dye samples. Discrimination was possible in water due to the robust nature of the IFE, avoiding the inherent challenges associated with systems operating through traditional host-guest interactions in aqueous media. The synthetic approach of copolymerization produced an easily tuneable platform, as various comonomers could tune the spectral regions in which the polymers absorb and emit light. This work could be extended to detect a diverse range of colored textile dyes and other optically dense compounds by designing fluorescent polymers to exhibit optical transitions in regions of interest. These results expand upon previous work in the Azoulay Research Group by broadening the utility of CP array-based sensing strategies to a wider range of analytes that are otherwise inaccessible through traditional energy transfer and aggregation-based approaches.

References

1. Kumar, A.; Kim, H.; Hancke, G., Environmental Monitoring Systems: A Review. *Sensors Journal, IEEE* **2013,** *13*, 1329-1339.
2. Sousa, J. C. G.; Ribeiro, A. R.; Barbosa, M. O.; Pereira, M. F. R.; Silva, A. M. T., A review on environmental monitoring of water organic pollutants identified by EU guidelines. *J. Hazard. Mater.* **2018,** *344*, 146-162.
3. Behmel, S.; Damour, M.; Ludwig, R.; Rodriguez, M. J., Water quality monitoring strategies — A review and future perspectives. *Sci. Total Environ.* **2016,** *571*, 1312-1329.
4. Madrid, Y.; Zayas, Z. P., Water sampling: Traditional methods and new approaches in water sampling strategy. *Trends Anal. Chem.* **2007,** *26*, 293-299.
5. Hilton, J.; Carrick, T.; Rigg, E.; Lishman, J. P., Sampling strategies for water quality monitoring in lakes: The effect of sampling method. *Environ. Pollut.* **1989,** *57*, 223-234.
6. Banna, M. H.; Imran, S.; Francisque, A.; Najjaran, H.; Sadiq, R.; Rodriguez, M.; Hoorfar, M., Online Drinking Water Quality Monitoring: Review on Available and Emerging Technologies. *Crit. Rev. Env. Sci. Tec.* **2014,** *44*, 1370-1421.
7. Storey, M. V.; van der Gaag, B.; Burns, B. P., Advances in on-line drinking water quality monitoring and early warning systems. *Water Res.* **2011,** *45*, 741-747.
8. Puvaneswari, N.; Muthukrishnan, J.; Gunasekaran, P., Toxicity assessment and microbial degradation of azo dyes. *Indian J. Exp. Biol.* **2006,** *44*, 618-626.
9. Chequer, F. M. D.; Oliveira, G. A. R. d.; Ferraz, E. R. A. c.; Cardoso, J. C.; Zanoni, M. V. B.; Oliveira, D. P. d., Textile Dyes: Dyeing Process and

Environmental Impact. In *Eco-Friendly Textile Dyeing and Finishing*, Günay, M., Ed. 2013.

10. Otero, P.; Saha, S. K.; Hussein, A.; Barron, J.; Murray, P., Simultaneous Determination of 23 Azo Dyes in Paprika by Gas Chromatography-Mass Spectrometry. *Food Anal. Methods* **2017,** *10*, 876-884.
11. Pielesz, A.; Baranowska, I.; Rybak, A.; Włochowicz, A., Detection and Determination of Aromatic Amines as Products of Reductive Splitting from Selected Azo Dyes. *Ecotox. Environ. Safe.* **2002,** *53*, 42-47.
12. Voyksner, R. D.; Straub, R.; Keever, J. T.; Freeman, H. S.; Hsu, W.-N., Determination of aromatic amines originating from azo dyes by chemical reduction combined with liquid chromatography/mass spectrometry. *Environ. Sci. Technol.* **1993,** *27*, 1665-1672.
13. Thomas, S. W.; Joly, G. D.; Swager, T. M., Chemical Sensors Based on Amplifying Fluorescent Conjugated Polymers. *Chem. Rev.* **2007,** *107*, 1339-1386.
14. Kubik, S., Anion recognition in water. *Chem. Soc. Rev.* **2010,** *39*, 3648-3663.
15. Langton, M. J.; Serpell, C. J.; Beer, P. D., Anion Recognition in Water: Recent Advances from a Supramolecular and Macromolecular Perspective. *Angew. Chem. Int. Ed.* **2016,** *55*, 1974-1987.
16. Chen, S.; Yu, Y.-L.; Wang, J.-H., Inner filter effect-based fluorescent sensing systems: A review. *Anal. Chim. Acta* **2018,** *999*, 13-26.
17. Tanwar, A. S.; Patidar, S.; Ahirwar, S.; Dehingia, S.; Iyer, P. K., "Receptor free" inner filter effect based universal sensors for nitroexplosive picric acid using two

polyfluorene derivatives in the solution and solid states. *Analyst* **2019,** *144*, 669-676.

18. Wu, M.; Sun, L.; Miao, K.; Wu, Y.; Fan, L.-J., Detection of Sudan Dyes Based on Inner-Filter Effect with Reusable Conjugated Polymer Fibrous Membranes. *ACS Appl. Mater. Interfaces* **2018,** *10*, 8287-8295.
19. Li, Z.; Askim, J. R.; Suslick, K. S., The Optoelectronic Nose: Colorimetric and Fluorometric Sensor Arrays. *Chem. Rev.* **2019,** *119*, 231-292.
20. Tropp, J.; Ihde, M. H.; Williams, A. K.; White, N. J.; Eedugurala, N.; Bell, N. C.; Azoulay, J. D.; Bonizzoni, M., A sensor array for the discrimination of polycyclic aromatic hydrocarbons using conjugated polymers and the inner filter effect. *Chem. Sci.* **2019,** *10*, 10247-10255.
21. Huang, F.; Wang, X.; Wang, D.; Yang, W.; Cao, Y., Synthesis and properties of a novel water-soluble anionic polyfluorenes for highly sensitive biosensors. *Polymer* **2005**, *46*, 12010-12015.
22. Li, Z.; Acharya, R.; Wang, S.; Schanze, K. S., Photophysics and Phosphate Fluorescence Sensing by Poly(phenylene ethynylene) Conjugated Polyelectrolytes with Branched Ammonium Side Groups. *J. Mater. Chem. C.* **2018,** *6*, 3722-3730.
23. Zhao, X.; Schanze, K. S., Fluorescent Ratiometric Sensing of Pyrophosphate via Induced Aggregation of a Conjugated Polyelectrolyte. *Chem. Commun.* **2010,** *46*, 6075-6077.
24. Chung, K.-T., Azo dyes and human health: A review. *J. Environ. Sci. Health C* **2016,** *34*, 233-261.

25. Brown, M. A.; De Vito, S. C., Predicting azo dye toxicity. *Crit. Rev. Env. Sci. Tec.* **1993,** *23*, 249-324.

26. Asses, N.; Ayed, L.; Hkiri, N.; Hamdi, M., Congo Red Decolorization and Detoxification by Aspergillus niger: Removal Mechanisms and Dye Degradation Pathway. *BioMed Res. Int.* **2018,** *2018*, 3049686-3049686.

27. Albert, K. J.; Lewis, N. S.; Schauer, C. L.; Sotzing, G. A.; Stitzel, S. E.; Vaid, T. P.; Walt, D. R., Cross-Reactive Chemical Sensor Arrays. *Chem. Rev.* **2000,** *100*, 2595-2626.

28. Röck, F.; Barsan, N.; Weimar, U., Electronic Nose: Current Status and Future Trends. *Chem. Rev.* **2008,** *108*, 705-725.

29. Liu, Y.; Bonizzoni, M., A Supramolecular Sensing Array for Qualitative and Quantitative Analysis of Organophosphates in Water. *J. Am. Chem. Soc.* **2014,** *136*, 14223-14229.

30. Puchtler, H.; Sweat, F.; Gropp, S., An investigation into the relation between structure and fluorescence of azo dyes. *J. R. Microsc. Soc.* **1967,** *87*, 309-328.

31. Instrumentation for Fluorescence Spectroscopy. In *Principles of Fluorescence Spectroscopy*, Lakowicz, J. R., Ed. Springer US: Boston, MA, 2006; pp 27-61

32. Tanwar, A. S.; Adil, L. R.; Afroz, M. A.; Iyer, P. K., Inner Filter Effect and Resonance Energy Transfer Based Attogram Level Detection of Nitroexplosive Picric Acid Using Dual Emitting Cationic Conjugated Polyfluorene. *ACS Sens.* **2018,** *3*, 1451-1461.

33. Tanwar, A. S.; Hussain, S.; Malik, A. H.; Afroz, M. A.; Iyer, P. K., Inner Filter Effect Based Selective Detection of Nitroexplosive-Picric Acid in Aqueous

Solution and Solid Support Using Conjugated Polymer. *ACS Sens.* **2016,** *1*, 1070-1077.

34. Şen, S.; Demirer, G. N., Anaerobic treatment of real textile wastewater with a fluidized bed reactor. *Water Res.* **2003,** *37*, 1868-1878.
35. Nguyen, T.; Saleh, M. A., Detection of azo dyes and aromatic amines in women undergarment. *J. Environ. Sci. Heal. A* **2016,** *51*, 744-753.